International Journal for Parasitology 52 (2022) 799–813

Contents lists available at ScienceDirect

International Journal for Parasitology

journal homepage: www.elsevier.com/locate/ijpara

Longitudinal transcriptome analysis of cattle infected with *Theileria parva*

M. Chepkwony [a,1], D. Wragg [b,1], P. Latré de Laté [a], E. Paxton [b], E. Cook [a], G. Ndambuki [a], P. Kitala [c], P. Gathura [c], P. Toye [a,*,2], J. Prendergast [b,*,2]

[a] Centre for Tropical Livestock Genetics and Health (CTLGH), ILRI Kenya, P.O. Box 30709, Nairobi 00100, Kenya
[b] Centre for Tropical Livestock Genetics and Health (CTLGH), Easter Bush Campus, EH25 9RG, UK
[c] College of Agriculture and Veterinary Sciences (CAVS), University of Nairobi, P.O. Box 29053-00624, Kangemi, Nairobi, Kenya

ARTICLE INFO

Article history:
Received 8 February 2022
Received in revised form 1 July 2022
Accepted 14 July 2022
Available online 13 October 2022

Keywords:
RNA
Gene expression
Host
Parasite
Boran
Tolerance
Theileria

ABSTRACT

The apicomplexan cattle parasite *Theileria parva* is a major barrier to improving the livelihoods of smallholder farmers in Africa, killing over one million cattle on the continent each year. Although exotic breeds not native to Africa are highly susceptible to the disease, previous studies have illustrated that such breeds often show innate tolerance to infection by the parasite. The mechanisms underlying this tolerance remain largely unclear. To better understand the host response to *T. parva* infection we characterised the transcriptional response over 15 days in tolerant and susceptible cattle (n = 29) naturally exposed to the parasite. We identify key genes and pathways activated in response to infection as well as, importantly, several genes differentially expressed between the animals that ultimately survived or succumbed to infection. These include genes linked to key cell proliferation and infection pathways. Furthermore, we identify response expression quantitative trait loci containing genetic variants whose impact on the expression level of nearby genes changes in response to the infection. These therefore provide an indication of the genetic basis of differential host responses. Together these results provide a comprehensive analysis of the host transcriptional response to this under-studied pathogen, providing clues as to the mechanisms underlying natural tolerance to the disease.

1. Introduction

The apicomplexan parasite *Theileria parva* infects cattle and buffalo, causing a fatal lymphoproliferative disease in the former, known as either East Coast Fever (ECF) or Corridor disease. ECF is transmitted from cattle to cattle by the tick *Rhipicephalus appendiculatus*, while Corridor disease occurs when the parasite is transmitted from buffalo to cattle by the same vector (Nene and Morrison, 2016; Cook et al., 2021). In susceptible animals, fatality rates from the diseases are over 90%, causing an estimated economic impact of over US $300 million annually to African farmers (Mukhebi, A. W., Perry, B.D., 1992. Economic implications of the control of East Coast fever in eastern, central and southern Africa, in: Proceedings of the Workshop, Zimbabwe; Tretina et al., 2015). However, previous work has illustrated that several native African breeds show elevated survival following exposure to the disease, suggestive of genetic tolerance. For instance, Ndungu et al. (2005) reported differential susceptibility of different cattle breeds in Kenya to the infection, with exotic and improved cattle breeds being more susceptible than indigenous cattle breeds. More recently, tolerance has been observed within a line of Boran cattle exposed to *T. parva* (Sitt et al., 2015; Latre de Late et al., 2021) and a genomic region of approximately 6 Mbp has been shown to be highly associated with the tolerance phenotype in these cattle (Wragg et al., 2022).

Previous studies of ECF have described the pathogenesis in detail (Lawrence et al., 2004), in addition to changes in parasite gene expression during infection (Bishop et al., 2005; Tonui et al., 2018; Atchou et al., 2020). As with other apicomplexan parasites, the *Theileria* spp. are known to hijack host gene expression during infection. By co-opting host cellular pathways of infected T and B cells, the parasites can transform the host cells and induce uncontrolled proliferation. Key host targets include repression of the NF-κB apoptotic pathway and elevated expression of metalloproteases that have been linked to invasion. Studies on the involvement of host genes during infection have largely focused on specific candidate genes within these pathways (Eichhorn et al., 1990; Heussler

* Corresponding authors.
E-mail addresses: p.toye@cgiar.org (P. Toye), james.prendergast@roslin.ed.ac.uk (J. Prendergast).
[1] Maurine Chepkwony and David Wragg contributed equally to this work.
[2] Philip Toye and James Prendergast contributed equally to this work.

https://doi.org/10.1016/j.ijpara.2022.07.006
0020-7519/

et al., 2001; Dessauge et al., 2005a; Tretina et al., 2020) and little is known of the genome-wide host transcriptional response during *T. parva* infection. Further understanding host transcriptional changes is likely to provide important insights into the effects of infection and how the host responds.

Understanding of *T. parva* pathogenetic processes has benefitted considerably from studies on the related parasite *Theileria annulata* which also infects cattle and immortalises infected cells. *Theileria annulata* infects and transforms B cells and monocytes whereas *T. parva* transforms T cells and B cells, with infected T cells being considered the more pathogenic (Emery et al., 1988; Spooner et al., 1989; Morrison et al., 1996; Tindih et al., 2012). As a result, the pathways involved in host cell infection and transformation may differ due to the cell types involved. An example is the interferon production by infected cells. Interferon (IFN) gamma (IFNγ) production has been associated with *T. parva*-infected T cells only, while *T. annulata*-infected cells have been associated with IFNß production (Ahmed et al., 1993; Sager et al., 1998).

As well as informing its role in cattle disease, the study of *T. parva* infection has relevance to human diseases. *Theileria parva* is related structurally and functionally to other apicomplexan parasites including the *Plasmodium* spp. that cause malaria. *Theileria parva* infects lymphocytes, immortalising them into exponentially dividing lymphoblasts with metastatic capacity similar to that of cancerous cells (Fry et al., 2016; Tretina et al., 2020). *Theileria parva*-transformed cells share a range of hallmarks with cancer cells which influence the pathogenesis of the infection including, for example, impairment of the apoptotic process, contributing to the immortalization of infected cells (Heussler et al., 1999). Similarly, the exponential proliferation of infected cells is another hallmark shared between *T. parva*-infected cells and cancer cells. This has been associated with production of certain cytokines that mediate this process, in addition to changes in the transcription factors involved in regulation of the cell cycle (Eichhorn et al., 1990; Dobbelaere et al., 2000; Heussler et al., 2001; Tretina et al., 2020). It has been proposed that a better understanding of host-*Theileria* interactions may identify cancer drugs that can be co-opted to treat *Theileria* infection as well as, potentially, provide insights into the shared mechanisms underlying cellular immortalization (Tretina et al., 2015).

Here, we characterise the transcriptional response in cattle across the course of natural infection with buffalo-derived *T. parva*. This study investigates changes in the expression of host genes during infection and associated biological pathways. In addition, we compare gene expression profiles between animals that survived infection and those that succumbed, providing insights into potential mechanisms underlying tolerance to infection.

2. Materials and methods

The study protocols were approved by the International Livestock Research Institute (ILRI, Kenya) Institutional Animal Care and Use Committee (Reference 2018–10).

2.1. Field challenge and sampling

In 2018, 30 Boran cattle from the Kapiti research station in Machakos county, Kenya, a region of low *T. parva* prevalence, were transported to the Ol Pejeta Conservancy (Nanyuki, Kenya) where they were naturally exposed to buffalo-derived *T. parva*. The cattle were part of an ongoing study investigating genetic tolerance to ECF, and their pedigree was known. Cattle were tested by ELISA using an established protocol to ensure no prior exposure to *Theileria mutans* and *T. parva* infection (Katende et al., 1998). While at Ol Pejeta, cattle were kept in an area of the ranch free from other cattle, but in the presence of buffalo. Whole blood samples were collected in 10 ml EDTA tubes prior to transporting cattle to Ol Pejeta (day 0) and exposure to *T. parva*, to characterise innate differences between the cattle. Additional blood sampling was conducted on days 7 and 15 of the trial to compare differences in transcriptome profiles during infection. Infection with *T. parva* was confirmed by microscopy of lymph node smears.

2.2. Isolation of white blood cells (WBCs) and RNA

Blood (4–5 ml) was transferred into 15 ml falcon tubes containing 10 ml of red blood cell lysis buffer (tris NH4CL2) and incubated at room temperature (RT) for 5 min. Tubes were then centrifuged at 300 *g* for 5 min at RT and the supernatant discarded. The pellet was rinsed twice with 15 ml of PBS and centrifuged at 300*g* for 5 min each time. The pellet was resuspended in 1.4 ml of tri-reagent, mixed using a pipette to form a homogenous lysate, and a 0.7 ml aliquot incubated at RT for 5 min before being stored at –20 °C. At the end of the field trial, samples were transferred to ILRI Nairobi and stored at –80 °C until RNA extraction.

RNA was extracted by phenol chloroform extraction as follows. The WBCs in tri-reagent were thawed at RT, vortexed briefly to homogenise the lysate, 0.2 ml of chloroform was added and left to incubate at RT for 3 min before being centrifuged for 15 min at 12,000*g* at 4 °C. The aqueous phase containing the RNA was collected by pipette and transferred into a sterile microtube, to which 1.5 ml of isopropanol was added and left to incubate at RT for 10 min. The sample was then centrifuged for 10 min at 12,000 *g* at 4°C and the supernatant discarded. The pellet was resuspended in 1 ml of 75% ethanol, vortexed briefly, centrifuged for 5 min at 7500 *g* at 4°C, supernatant discarded, and pellet left to dry for 10 min before resuspending in RNAse-free water. RNA quality was assessed by a NanoDrop™ spectrophotometer to ensure an A230/280 ratio >1.8, and by running the sample on a 1.5% agarose gel to check for the presence of 28S, 18S, mRNA and micro-RNA bands. Samples were shipped on dry ice to the Roslin Institute in the UK.

2.3. Processing of RNA-seq data

Library preparation (TruSeq Stranded mRNA) and sequencing of RNA samples was performed by Edinburgh Genomics (UK) on the Illumina HiSeq platform. Each sample was sequenced across three lanes with a target coverage of 70 M × 50 bp reads per sample. Sample sequencing qualities were assessed using fastQC (v0.11.7) (Andrews, S., 2010, FastQC: A Quality Control Tool for High Throughput Sequence Data, https://www.bioinformatics.babraham.ac.uk/projects/fastqc/). Reads were aligned to the *Bos taurus* ARS-UCD1.2 genome assembly (https://ftp.ensembl.org/pub/release-97/fasta/bos_taurus/dna/Bos_taurus.ARS-UCD1.2.dna.toplevel.fa.gz) using STAR (v2.7.1a; --sjdbOverHang 49 --genomeSAindexNbases 14) (Dobin et al., 2013), for which the ARS-UCD1.2 gene annotation file (https://ftp.ensembl.org/pub/release-97/gtf/bos_taurus/Bos_taurus.ARS-UCD1.2.97.gtf.gz) was also provided. Unmapped reads were subsequently aligned to the *T. parva* ASM16536v1 genome assembly (https://ftp.ncbi.nlm.nih.gov/genomes/all/GCF/000/165/365/GCF_000165365.1_ASM16536v1/GCF_000165365.1_ASM16536v1_genomic.fna.gz) using STAR (--sjdbOverHang 49 --genomeSAindexNbases 10). The resulting sample alignment qualities were assessed using fastQC. Per base sequence content from the fastQC reports were analysed in R. Gene GC content was retrieved within R (v4.0.2) from Ensembl's BioMart (Ensembl Genes 104; btaurus_gene_ensembl; version ARS-UCD1.2) with the biomartr package (Drost and Paszkowski, 2017). Functional profiling of genes in the upper and lower 5% of the distribution of log normalised gene expression

ratios (day 15/day 0), from equal content-sized bins of day 0 gene expression, was performed using the g:GOSt tool of g:Profiler (Raudvere et al., 2019). All expressed genes were provided as the custom domain space, the query list of genes was ordered by log normalised gene expression ratio, and an ordered query performed with the g:SCS algorithm (Reimand et al., 2007).

Non-parametric Wilcoxon tests were used in Figs. 1 and 2 as the underlying data was generally not normally distributed.

2.4. Differential gene expression analyses

Mapped reads were summarised using featureCounts (-F "GTF" -t "exon" -g "gene_id") (Liao et al., 2014). The gene counts were then analysed for differential gene expression using the DESeq2 R package (Love et al., 2014). We ran a likelihood ratio comparison between the full model with an interaction term between day and status (design = ~day + sex + group + status + day:status) and a reduced model (reduced = ~day + sex + group). Covariate factors were sex (male (M) or female (F)), day (0, 7, or 15), and group (pedigree or unrelated), while status was a binary indicator of survival outcome. We also fit independent models for each day (design = ~sex + group + status) and compared those with a reduced model (reduced = ~sex + group). Model comparisons were performed using likelihood ratio tests (LRTs).

Log_2 fold change and *P* value outputs were considered for the description of differentially expressed genes (DEGs). We explored genes that were significantly differentially expressed at a false discovery rate (FDR) of ≤0.05 as well as those that were differentially expressed at a nominal *P* value of <0.01, or had a log_2 fold change >1. The gene lists generated from these comparisons were used for gene set enrichment analyses (GSEA). LRT results for these genes were clustered using the hierarchical clustering implementation tool DEGreport (Piper, M., Khetani, R., Daily, K., Perumal, T.M., Kirchner, R., Steinbaugh, M., 2021. DEGreport: Report of DEG analysis. Bioconductor version: Release (3.14). https://doi.org/10.18129/B9.bioc.DEGreporthttps://doi.org/10.18129/B9.bioc.DEGreport).

2.5. eQTL and reQTL analyses

Statistical modelling was performed in R (v4.0.2). Expression quantitative trait loci (eQTL) analyses were performed using DESeq2 normalised gene expression values and Illumina BovineHD genotype data generated by Wragg et al. (2022). To identify eQTL within each time point for each gene and *cis* variant we fitted a linear model of gene expression against allele dosage at the *cis* variant, accounting for sex (M or F) and group (pedigree or unrelated) as factors. A *cis* variant included any bi-allelic variant within 1 Mb upstream and 1 Mb downstream of the start and end positions, respectively, of the gene, with a minor allele frequency >0.1. Within each time point we adjusted the eQTL F-statistic *P* values to FDRs. From the eQTL models we sought to identify response eQTL (reQTL) by performing a beta-comparison of regression slopes. Briefly, regression coefficients (β) and variance (σ) were calculated for each eQTL and compared between time points using a z-test:

$$z = \frac{\beta_a dayA - \beta_b dayB}{\sqrt{\sigma^2 dayA + \sigma^2 dayB}}$$

2.6. Functional enrichment analyses

We employed the Database for Annotation, Visualisation, and Integrated Discovery (DAVID), functional annotation tool (Huang et al., 2009) to test for functional enrichment. This was further supplemented by analysis of the same genes using the Functional Mapping and Annotation of Genome-Wide Association Studies (FUMA-GWAS) tool (Watanabe et al., 2017) using the Gene2Func function.

2.7. Data availability

RNA sequencing data is available to download from the European Nucleotide Archive under project accession PRJEB39210. Illumina BovineHD genotype data is available to download from Edinburgh DataShare, https://doi.org/10.7488/ds/2985.

3. Results

Pedigree, gender and survival details for the animals in the study are provided in Supplementary Table S1. One animal was killed by a lion on day 9 of the trial and thus was lost to follow-up study. We analysed the transcriptional response of the remaining 29 Boran cattle exposed to field infection with *T. parva*. Among them, 23 were progeny of three sibling sires (sire 1, *n* = 5; sire 2, *n* = 9; sire 3, *n* = 9), which we refer to below as "pedigree" animals, while six were unrelated. In total, 20 cattle succumbed to infection (dead, treated or euthanised) while nine cattle survived without intervention. The mean time to death or intervention was 20.4 days. Some samples for a given time point did not produce sequence data due to low RNA integrity number (RIN) scores, giving a total of 28, 23 and 28 samples at days 0, 7 and 15, respectively.

3.1. Transcriptome base sequence content diverges post-infection

Analysis of *B. taurus*-aligned reads revealed a marked global transcriptional response during the 15 days following translocation to the field site, with a clear shift in the GC content of transcribed genes (Fig. 1A). Whereas the median GC content of transcripts expressed at day 0 was 50.9 ± 4.24 S.D., this increased to 54 ± 4.15 on day 7, and 55 ± 3.99 on day 15 (Wilcoxon rank sum test: $P < 0.05$, Fig. 1B). Breaking down genes by their expression levels on day 0 highlighted that highly expressed genes with a low GC content are more likely to decrease in their relative expression levels over the course of the infection (Fig. 1C,D). These results indicate a general transcriptional response to infection linked to the GC content of genes.

To further illustrate this, we undertook functional analysis of highly expressed genes (Fig. 1D) with a log normalised expression ratio (day 15/day 0) in the upper or lower 5% of the distribution, and which had a low (≤41.7) or high (≥51.1) GC content. In particular, we found significant enrichment (g:SCS adjusted $P < 0.05$) of the thymic stromal lymphopoietin (TSLP) and transforming growth factor-β (TGF-β) signalling pathways among low GC content genes exhibiting a reduction in relative expression, and for a range of immune-related terms among high GC content genes exhibiting an increase in relative expression (Supplementary Tables S2–S5).

3.2. Analysis of unmapped reads confirms T. parva infection

Reads that failed to align to the *B. taurus* genome were aligned to the *T. parva* genome to study parasite expression. We observed a 20-fold increase in the proportion of these reads that aligned to the *T. parva* genome from background levels on day 0, (median 3562 ± 3762 S.D. reads) to day 15 (median 71511 ± 124551). The relative increases in the proportion of *T. parva*-aligned reads were significant at both day 7 (Wilcoxon rank sum test: $P = 0.0084$) and day 15 (Wilcoxon rank sum test: $P = 1 \times 10^{-15}$; Fig. 2A). Comparing the day 15 proportion of *T. parva*-derived reads between animals

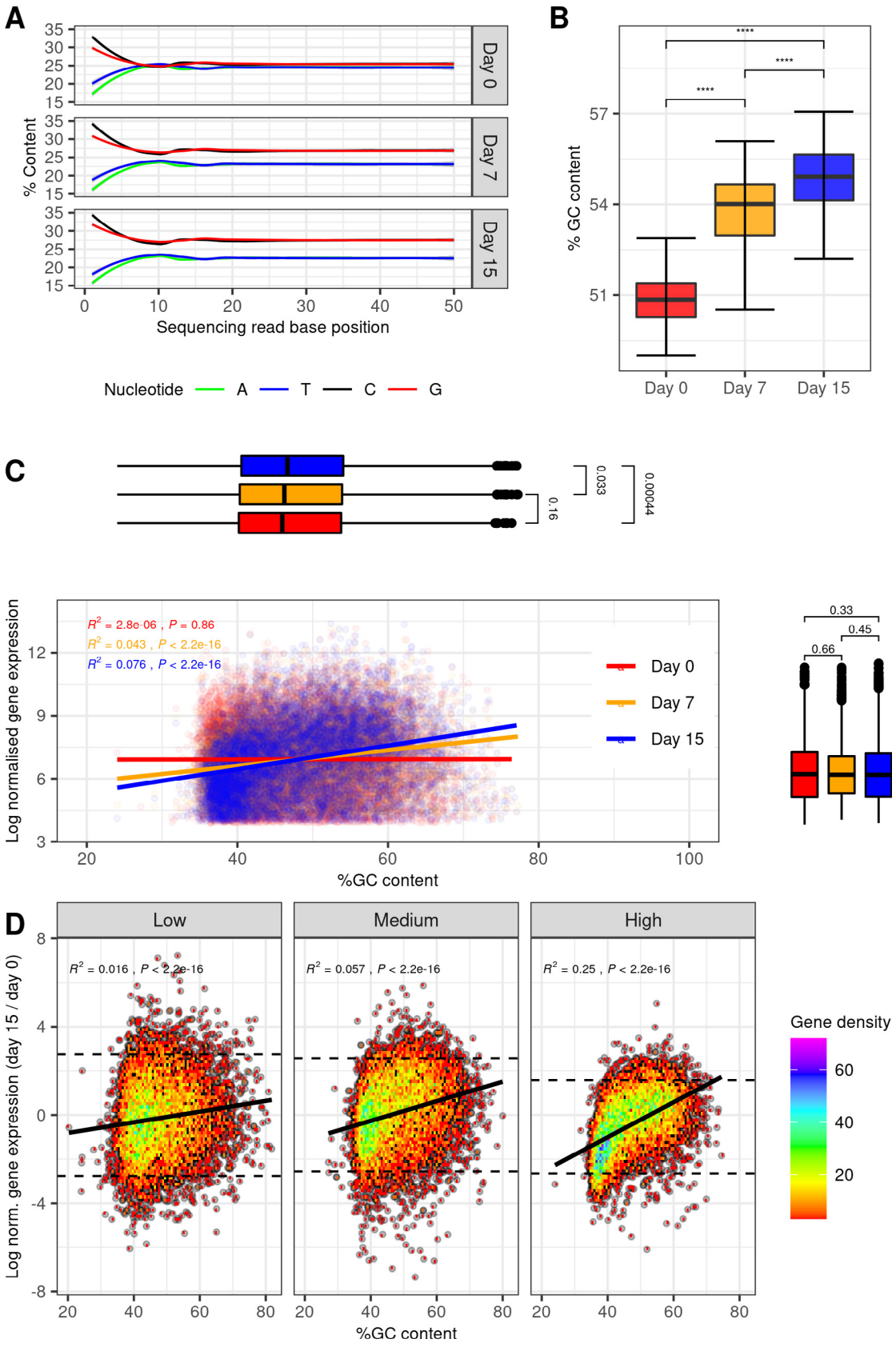

Fig. 1. Global change in transcript sequence content divergence following infection in Boran cattle by *Theileria parva*. (A) Median nucleotide base sequence content across samples at days 0, 7 and 15. (B) Comparison of GC content across base positions 20 to 40 between days 0, 7 and 15. The difference in GC content was significant (Wilcoxon rank sum test: $^{****}P < 2.2 \times 10^{-16}$) in all comparisons. (C) Genes with expression levels exceeding the 50th percentile for each day, plotted as log normalised expression against the percentage of GC content, with regression lines showing an increase in GC content of these most highly expressed genes post-infection. Marginal box plots indicate a significant shift in GC content (Wilcoxon rank sum test: $P < 0.05$) post-infection. (D) Genes were grouped into three equal content-sized bins based on day 0 expression levels (low, medium, high), and the ratio of normalised expression levels between days 15 and 0 logged and plotted against GC content, confirming the relationship between GC content and expression level change, particularly among the genes more highly expressed pre-infection. Horizontal dashed lines in D indicate the 5th and 95th percentiles of the normalised expression data.

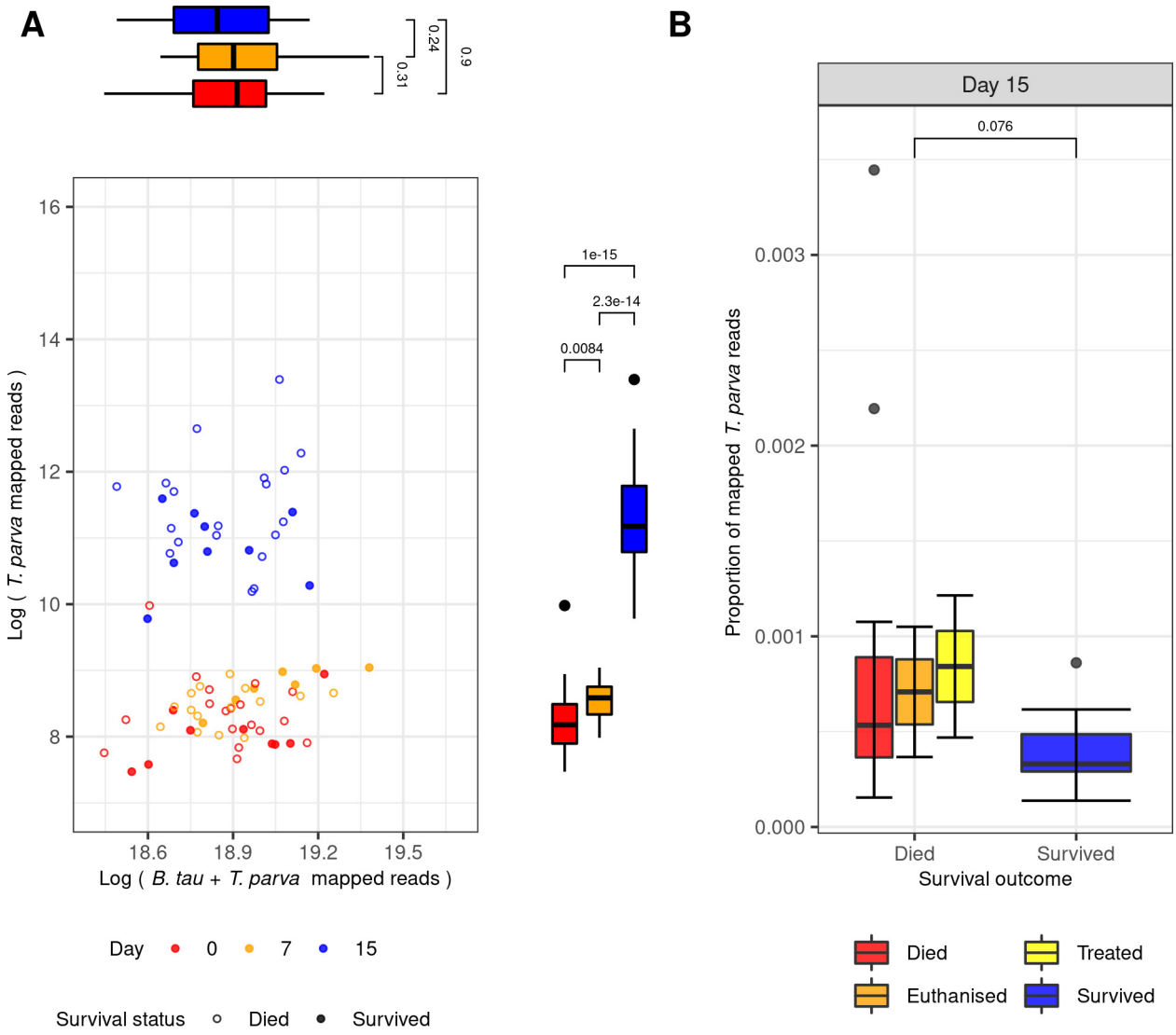

Fig. 2. Proportion of reads mapping to the *Theileria parva* genome relative to all reads mapped (i.e. to both *Bos taurus* and *T. parva* genomes). (A) The $\log_{10}$ number of reads mapped to the *T. parva* genome versus all reads mapped. Differences in the total number of reads mapped between time points were not significant, whereas there was a significant difference in the number of reads mapping to *T. parva* between each time point, with the most significant increase from day 0 to day 15 (Wilcoxon rank sum test: $P = 1 \times 10^{-15}$). (B) The proportion of reads mapped to the *T. parva* genome grouped by survival outcome. Comparison of means between animals that succumbed or were treated and those that survived infection returns a Wilcoxon *P* of 0.076.

that died ($n = 15$), were treated ($n = 2$) or euthanised ($n = 2$) due to severe illness, and those that survived ($n = 9$) returned a Wilcoxon *P* value of 0.076, with survivors possessing, on average, the smallest proportion of *T. parva*-derived reads (Fig. 2B).

3.3. Host genes change in expression pattern throughout the course of the field trial

A principal component analysis (PCA) of normalised bovine gene expression levels revealed both a clear differentiation of samples collected before and after exposure to *T. parva* along PC1, and divergence between samples collected at days 7 and 15 on PC2 (Fig. 3). To identify genes differentially expressed across the course of infection (DEGs) a time course analysis across the three timepoints (days 0, 7 and 15) was carried out. When accounting for survival status, sex, and relatedness (pedigree or unrelated), DEGs significant at FDR < 0.05 clustered into four groups (Fig. 4A) which can broadly be described as: (1) genes with relatively high expression on day 7 but reduced by day 15 (cluster 1, $n = 2603$); (2) genes that have higher expression on day 7 and remain so on day 15 (cluster 2, $n = 6095$); (3) genes that show a gradual increase in expression from day 0 to 15 (cluster 3, $n = 748$); and (4) genes with a lower relative expression at day 15 compared with day 0 (cluster 4, $n = 7238$).

Gene set enrichment analysis (GSEA) was performed to identify gene ontologies and pathways that were enriched across the genes within the different clusters (Table 1). A more detailed presentation of the data can be found in Supplementary Fig. S1. Many of the annotations identified are linked to the establishment of infection, cell proliferation, cell death or metastasis. Cytokine signalling through the Janus kinase-signal transducer and activator of transcription (JAK-STAT) pathways, among others, are highlighted. These include proinflammatory cytokines such as IL6, tumour necrosis factor (TNF) alpha (TNFα), IFNγ and IFNα, which have all been described to increase in production in *Theileria* infections (McGuire et al., 2004; Razmi et al., 2019), where they potentially contribute to survival, invasiveness, and metastasis of *Theileria*-transformed cells (Ma and Baumgartner, 2014). Some genes which

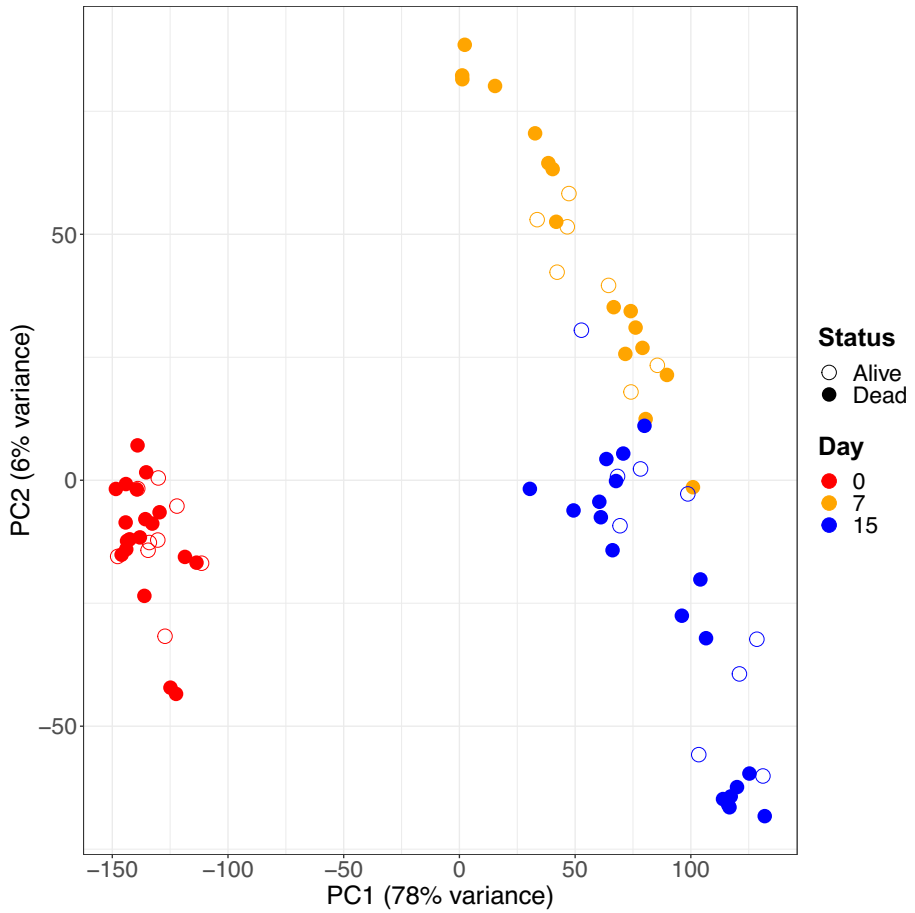

Fig. 3. Principal Components Analysis (PCA) of normalised gene expression data. Each circle represents a sample from an individual animal at a specific time point, as indicated.

are targets of either *E2F* or *MYC* are enriched among cluster 2 genes. *E2F*- and *MYC*-related pathways have been shown to play a role in enhancing survival and proliferation of *Theileria*-infected cells (Dessauge et al., 2005a; Tretina et al., 2020). The JAK/STAT3 signalling pathway has previously been suggested to contribute to *c-Myc* activation and is associated with host cell transformation by *Theileria* (Dessauge et al., 2005a), which is supported by our results showing that genes involved in IL6_JAK_STAT3 signalling pathway are differentially expressed on days 7 and 15. Other highlighted pathways included the tumour protein 53 (*P53*) and members of class O of forkhead box transcription factor (*FoxO*) signalling pathways - which have been associated with apoptosis of host proliferating cells (Haller et al., 2010; Aster et al., 2017). *P53* is a pro-apoptotic protein, expression of which is directly dependent on parasite interaction (Haller et al., 2010). In our study, *P53* shows higher expression (Fig. 4B) on days 7 and 15 compared with day 0. *P53* interacts with *TNFα*-activated nuclear factor kappa beta (*NFkB*) competitively and they inhibit each other's activities (Webster and Perkins, 1999; Dobbelaere et al., 2000). *TNFα* signalling via *NFkB*, which is enriched among cluster 3 genes, is not only involved in pro-apoptotic and pro-survival signals but also promotes invasiveness and metastasis of *Theileria*-transformed cells (Ma and Baumgartner, 2014). In this study, expression of NFkB was highest prior to infection by *T. parva*, and the number of transcripts reduced during the course of infection (Fig. 4B). This is contrary to previous results which described NFkB to be persistently induced by *T. parva* infection and required for T cell activation and proliferation (Palmer et al., 1997). Genes involved in IL2-STAT5 signalling are differentially expressed among cluster 1 genes. *IL2* is a primary growth factor for activated T cells in this pathway (Mahmud et al., 2013). We observed a marginal but non-significant increase in *IL2* expression at day 7, and a significant (Wilxocon rank sum test: $P < 0.05$) decrease by day 15, while *IL2* receptors (*IL2RA*, *IL2RB* and *IL2RG*) show a significant increase in expression at day 15 (Fig. 4C).

Enrichment analyses were conducted with FUMA and DAVID, and reported only where both tools returned a FDR < 0.05 in the categories: hallmark gene sets, Kyoto Encyclopaedia of Genes and Genomes (KEGG) pathways, Biocarta pathways, gene ontoloty (GO) biological processes (BP), GO cellular components (CC), and GO molecular functions (MF). Detailed results are presented in Supplementary Fig S1.

3.4. Expression patterns of certain genes differ in surviving and susceptible cattle

To investigate whether there was potentially a different transcriptional response in the animals that survived infection, we compared those that died, were euthanised or were treated, with those that survived and had cleared the parasite from their lymph node smears by the end of the trial without intervention (Fig. 2B, survived group). We identified 64 genes significantly differentially expressed between the dead and surviving cattle across the time-points at an FDR < 0.05. The majority of genes clustered into two groups, reflecting a reduction (cluster 1$n = 22$) or an increase (clus-

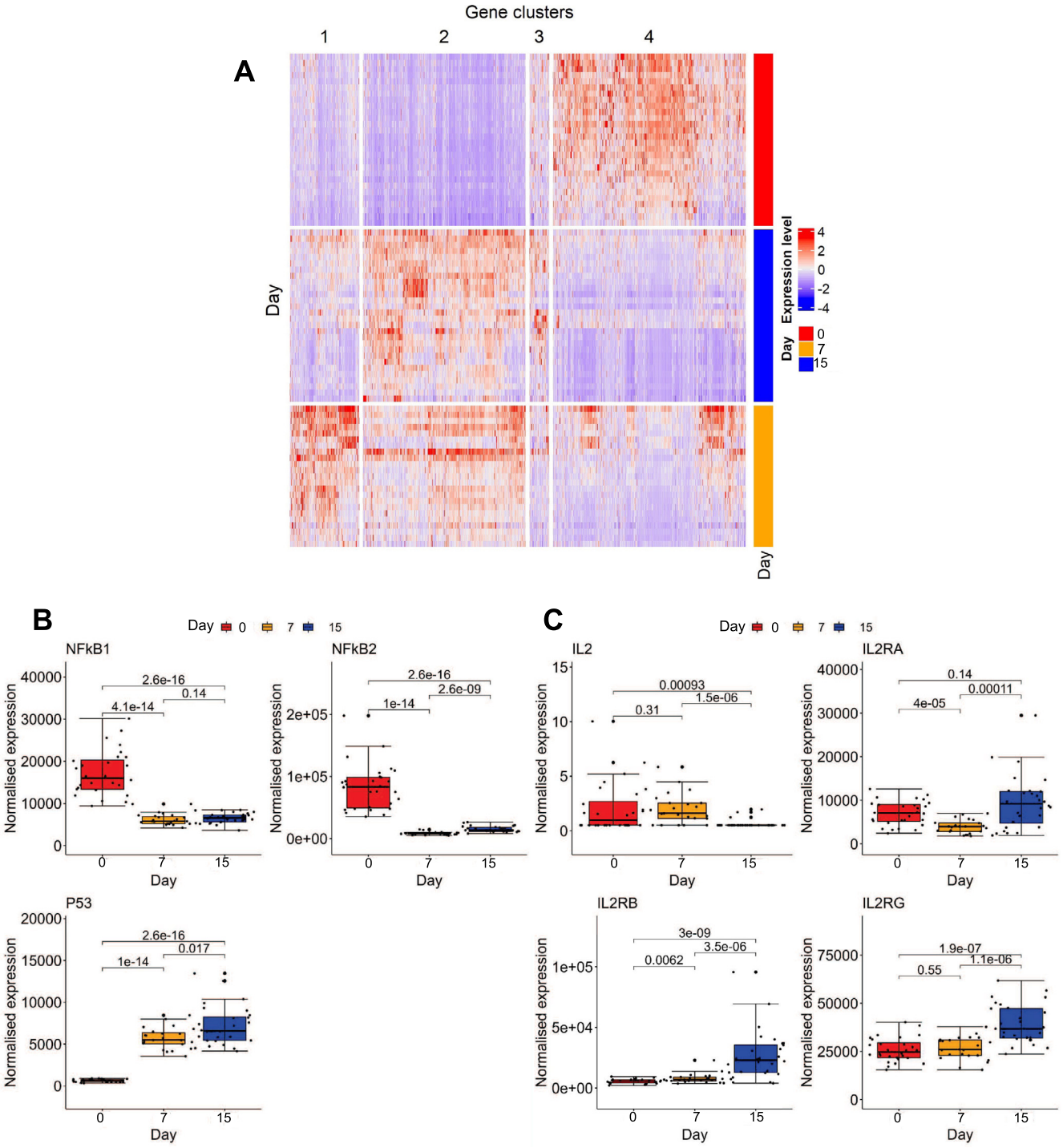

Fig. 4. Trends of host (*Bos indicus*) gene expression in response to field exposure to *Theileria parva*. (A) Heatmap of significantly differentially expressed genes across sampling time points. The heatmap is scaled by column with each row representing an individual sample and each column representing a gene. The genes cluster into four groups, as denoted above the heatmap. (B) Antagonistic expression patterns of nuclear factor kappa beta (*NFkB)* and tumour protein 53 (P53) proteins across the time course. (C) The expression patterns of interleukin (IL)2 and its receptors (IL2RA, IL2RB, IL2RG) across time.

ter $2n$ = 34) in expression levels following field exposure to infection.

The most significantly differentially expressed gene (FDR = 5.0×10^{-4}) was kinesin family member 12 (*KIF12*), which was expressed more highly in the surviving group on day 15. *KIF12* has been reported to play a critical role in cell division, specifically in cytokinesis (Lakshmikanth et al., 2004), and in the cellular response to oxidative stress (Yang et al., 2014). Other highly differentially expressed genes with known functions included RNA binding motif protein 3 (*RBM3*) for which high expression has been associated with increased survival rates for patients with certain types of cancers (Pilotte et al., 2018; Gao et al., 2020). Although in our analysis, expression of *RBM3* generally decreased following infection, its expression was higher in cattle that survived. Vasohibin1 (*VASH1*) inhibits proliferation and migration of endothelial cells, thus limiting the metastasis of tumour cells in cancers

Table 1
Biological functions/pathways were significantly enriched (false discovery rate adjusted $P \leq 0.05$) in gene clusters showing differential expression across time in *Theileria parva*-infected cattle.

Annotation	Pathways enriched in gene clusters (from Fig. 4A)			
	1	2	3	4
Complement	●			
Epithelial-mesenchymal transition	●			
Apical junction	●			
KRAS signalling	●			
IL2_STAT5 signalling	●		●	
Hypoxia	●			●
Oxidative phosphorylation		●		
MYC targets		●		
DNA replication		●		
Biosynthesis of amino acids		●		
Fatty acid metabolism		●		
Mitochondrial translation		●		
E2F		●		
Mitochondrion		●	●	
Nucleoplasm				●
Interferon gamma response		●	●	
Apoptotic process		●		
Ribonucleotide binding		●		●
T cytotoxic pathway		●		
MAPK pathway		●		
EDG1 pathway		●		
AHSP pathway		●		
TCR pathway		●		
Inflammatory response			●	
Cell response to lipopolysaccharide			●	
Allograft rejection			●	
Chemokine signalling pathway			●	
Interferon Alpha response			●	
IL6_JAK_STAT3 signalling			●	
TNFA signalling via NFKB			●	●
TGF beta signalling			●	
TH1TH2 pathway			●	
TID pathway			●	
Reck pathway			●	
Apoptosis				●
P53 pathway				●
Regulation of cell proliferation			●	
Defense response			●	

(Du et al., 2017; Zhao et al., 2017; Wang et al., 2019), as well as protecting endothelial cells from the effects of toxic stress (Miyashita et al., 2012). *VASH1* expression generally increased following infection and was significantly higher (FDR = 0.0012) in cattle that survived infection. High mobility group box 3 (*HMGB3*), which has been shown to have pro-proliferative and pro-metastatic effects in cancer cells (Nemeth et al., 2005, 2006; Guo et al., 2016; Liu et al., 2018), decreased in expression from day 0 to day 15 and was more highly expressed in surviving cattle. IFN-induced protein with tetratricopeptide repeats 1 (*IFIT1*) was the most upregulated gene in survivors among the significant DEGs (log2fold change = 3.73), followed by protein C receptor (*PROCR*) (Supplementary Table S6). *IFIT1* has roles in immune response, metastasis, and apoptosis, and has been described to have increased expression in cancers (Critchley-Thorne et al., 2007; McDermott et al., 2012; Wah et al., 2018; Pidugu et al., 2019) while certain alleles of the gene have been linked to better malaria prognosis (Wah et al., 2018). In our study, *IFIT* expression generally reduced across time but was higher in the survivors than those that subsequently died. Syntaxin-binding protein 1 (*STXBP1*) was the most downregulated gene among the significant DEGs ($\log_2$ fold change = −2.73) followed by purinergic receptor P2X3 (*P2RX3*; $\log_2$ fold change = −2.04), both of which follow the cluster 2 expression pattern across time. We performed GSEA on all 64 significant DEGs (Supplementary Table S6). Toll-like receptors (*TLRs*), protein kinase B (*AKT*) and mechanistic target of rapamycin kinase (*MTOR*) immunological functions and pathways were found to be enriched, and are widely reported to play a role in *T. parva* infection in the literature (Heussler et al., 2001; Chi, 2012; Kinnaird et al., 2013; Kamau et al., 2016; Saxton and Sabatini, 2017; Kim and Guan, 2019). *AKT* and *MTOR* enrichment was associated with four genes (*IFIT1*, *KCNE3*, *KLRB1* and *DLG4*), and although *AKT* and *MTOR* can interact, affecting cell survival (Hay and Sonenberg, 2004), they are not reported to interact directly with one another (based on a STRING db analysis (Szklarczyk et al., 2019)).

We next assessed genes that were differentially expressed between survivors and those that subsequently died at specific timepoints, rather than across the time-series as a whole. We ran a similar model using LRTs to identify differentially expressed genes associated with survival status at individual timepoints (days 0, 7 or 15) while accounting for sex and relatedness (pedigree or unrelated). No significant DEGs were found between these groups on day 0 at an adjusted *P* value of 0.05 (FDR). However, 141 genes were differentially expressed at a nominal *P* value of 0.01. We considered these as candidate genes that were innately differentially expressed (pre-infection with *T. parva*) between survivors and those that went on to succumb to infection. On day 7, 95 genes that were differentially expressed at a nominal *P* value of 0.01 were considered as genes that responded early to infection, none of which were significant after correcting for multiple testing. At day 15, we identified 11 DEGs (Table 2) with FDR < 0.05 and 596 genes with a nominal $P < 0.01$. Of the 11 DEGs with FDR < 0.05, six

Table 2
Significantly differentially expressed genes (false discovery rate adjusted $P < 0.05$) on day 15 between surviving animals and those that succumbed to infection. Gene names in parentheses are the human orthologs of cattle genes that remain to be annotated in the *Bos taurus* genome.

Gene stable ID	Gene name	Succumbed/survivors expression (fold change)	Adjusted *P* value
ENSBTAG00000047632	(IGHE)	0.16	4.54E-05
ENSBTAG00000049598	H2BC7	0.29	0.011
ENSBTAG00000054686	CRACDL	0.40	0.043
ENSBTAG00000001527	TMEM213	0.14	0.049
ENSBTAG00000048135	(IGHG2)	0.19	0.049
ENSBTAG00000004739	SLC18A2	0.23	0.049
ENSBTAG00000010742	PKD2L1	0.25	0.049
ENSBTAG00000015685	KIF12	0.26	0.049
ENSBTAG00000048257	(CYP4F22)	0.33	0.049
ENSBTAG00000007558	IL9R	0.42	0.049
ENSBTAG00000053829		0.49	0.049

(*IGHE*, *TMEM213*, *PKD2L1*, *KIF12*, *IL9R* and *ENSBTAG00000053829*; Fig. 5A–F) were also present among the overall significant DEGs shown in Supplementary Table S6.

Among the 11 genes displaying a difference between the animals that survived and succumbed at day 15, the most differentially expressed gene, ENSBTAG00000047632, is a novel gene orthologous (40.94%) to human immunoglobulin heavy constant epsilon (*IGHE*). Human IgE, the product of *IGHE*, has been observed to be upregulated in response to malaria (Duarte et al., 2007). These data suggest this gene shows a differential response in survivors and those that succumbed to *T. parva* infection. ENSBTAG00000048135 (Table 2), another novel gene, is orthologous to several human immunoglobulin heavy constant gamma genes (*IGH1*, 63.50%; *IGHG2*, 65.03%; *IGH3*, 62.58%; *IGH4*, 63.80%). *IGHG2* is the heavy chain of IgG2 immunoglobulin, expression of which has been associated with protecting individuals against infection with both malaria (Aucan et al., 2000) and *T. parva* (Musoke et al., 1982). Transmembrane protein 213 (*TMEM213*) has been associated with invasion and metastasis in cancers when downregulated and is considered an independent predictor of overall survival in lung cancer with individuals who survive longer showing higher expression of the gene (Zou et al., 2019). In our study, levels of *TMEM213* increased in all cattle across time, with survivors having a significantly higher abundance of the gene transcripts. Another notable gene identified is the receptor for IL9 (*IL9R*). IL9 can play both a tumorigenic role and antitumor role in cancers depending on the interacting molecules (Wan et al., 2020). We observed IL9 expression to generally reduce in all animals during the field challenge, with abundances being lower in the survivors - although this difference was not significant ($P = 0.7$, Fig. 5G).

3.5. Functional enrichment of genes differentially expressed in T. parva-tolerant cattle

DEGs with nominal $P \leq 0.01$ at each timepoint (days 0,7,15) were separated into lists where their expression was either (i) higher or (ii) lower in cattle that survived infection. Functional enrichment analyses were subsequently performed on each list independently, and the complete results are provided in Supplementary Table S7. Biological pathways and annotations exhibiting significant enrichment ($P\text{adj} \leq 0.05$) in surviving animals are presented in Fig. 6 for each time point. The IFNγ response was significantly enriched at all three timepoints with different gene sets being associated with the signal at each point (Supplementary Table S7). This suggests that the signalling pathway may be regulated differently between survivors and cattle that succumbed to infection, and that its effect at the various timepoints may vary depending on the receptors and molecules modulating it. Further investigation of gene interaction networks may help to elucidate the impact of infection by *T. parva* on the IFNγ response.

At day 0, the nominally significant ($P \leq 0.01$) gene set returned enrichment signals across genes that were more highly expressed in survivor cattle compared with those that succumbed to infection, but not for genes with lower expression levels in survivors. Several of the enriched signals returned were previously identified (Table 1), including IL2-STAT5 signalling, IFNα and IFNγ responses, interleukin-1β secretion, and positive regulation of the *NLRP3* inflammasome complex (Fig. 6). *IFIT3* was among four genes associated with an IFNα response and exhibited higher expression levels in survivors at day 0. Its expression profile was reversed by day 7, with average expression levels being higher in cattle that ultimately succumbed to infection, and by day 15 its expression returned to being higher on average in survivors. However, these differences were not significant after FDR adjustment. *IFIT3* can be induced by either IFNα or IFNγ, and it has been suggested that increased expression of *IFIT3* through *IFN* induction contributes to increased cell survival and a reduction in cellular apoptosis (Hsu et al., 2013).

At days 7 and 15, we observe various pathways enriched among genes with reduced expression at these timepoints in survivors relative to cattle that succumbed to infection (Fig. 6). These results show that some processes necessary for *T. parva* to infect, proliferate, and metastasize are associated with genes that are expressed at significantly lower levels in cattle that survive infection. The most enriched signal at day 15 was hypoxia, for which the functions of the three most significant genes (*SDC3*, *GPC1* and *PRKCA*) appear to be mediated through interaction with hypoxia inducible factor-1α (*HIF-1α*).

3.6. eQTL

To identify potential genetic drivers of expression differences between samples and timepoints we mapped eQTL and response eQTLs in the cohort. Here an eQTL is a genetic variant with genotypes that are correlated to the expression of a nearby gene at a given timepoint (Nica and Dermitzakis, 2013). To identify eQTLs, at each timepoint we fit models testing the association of each gene's expression with *cis* variants, while accounting for sex and relatedness (see section 2). Any variant within 1 Mb upstream of a gene's start position and 1 Mb downstream of a gene's end position was considered to be a *cis* variant. After correcting for multiple testing, the proportion of genes with an eQTL (FDR < 0.05) was significantly different between days (chi-sq: $P = 1.66 \times 10^{-37}$) with the number of genes identified at day 0 ($n = 316$) being greater than days 7 ($n = 86$) and 15 ($n = 115$), which collectively represented a total of 462 unique genes.

These data suggest the impact of genetic variants on gene expression may be changing over the course of the infection. To investigate this further, we characterised response eQTLs by comparing the coefficients of eQTLs between timepoints (see Section 2). The proportion of genes with a response eQTL (reQTL; $|Z| > 4$) was significantly different between pairs of days (chi-sq: $P = 3.48 \times 10^{-82}$), with the number of genes identified being greatest between days 0 and 15 ($n = 1626$), followed by day 0 versus day 7 ($n = 1282$), and day 7 versus day 15 ($n = 712$), representing a total of 1958 unique genes of which 233 were identified in the previous step as having a significant eQTL. An example of an reQTL associated with the *RTN4IP1* gene is presented in Fig. 7.

From the significant DEG lists relating to survival, 28 genes with a nominal $P < 0.01$ were also found to have one or more significant eQTL, which is significantly more than expected by chance (chi-sq: $P = 0.018$ comparing DEGs with significant eQTL to non-DEGs with

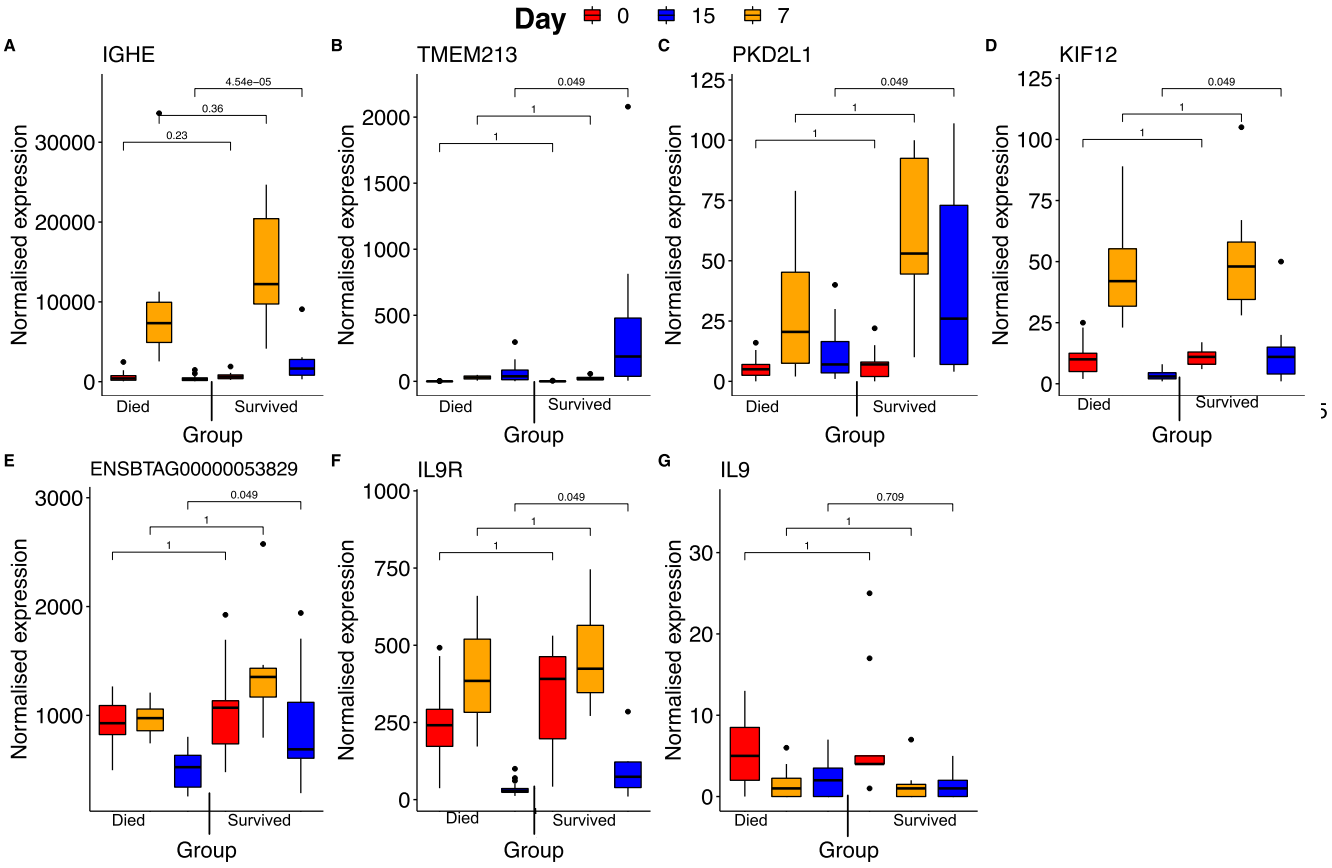

Fig. 5. Bar graphs showing expression profiles of select genes across time in cattle exposed to *Theileria parva*. (A–F) Expression profiles of the six genes significantly differentially expressed at false discovery rate adjusted $P < 0.05$ between the surviving and deceased animals at day 15 as well as across the entire time course. (G) Expression profile of IL9.

significant eQTL). These include *PKD2L1* which was the only DEG with FDR < 0.05 to have a significant eQTL (eQTL on day 15 FDR = 0.008). *VASH1* plays a role in cancer cell metastasis (Ito et al., 2013; Mikami et al., 2017) and had a significant reQTL between days 0 and 7 (Z = -6.2), and days 0 and 15 (Z = 6.5).

Functional enrichment of the 28 putative DEGs with significant eQTLs revealed enrichment for a single term: NOTCH signalling (cancer gene module of FUMA software). This signalling pathway was associated with four genes in our analysis: *PKD2L1*, *CLSTN3*, *MYO1A* and *HS1BP3*, which suggests that the dysregulation of the NOTCH signalling process in the immune response to *T. parva* infection is dependent on host genetics across these genes.

4. Discussion

This study describes differential expression of genes across time after field exposure to buffalo-derived *T. parva* infection. We report here genes that are differentially expressed in the bovine host and the associated functions enriched among the significantly differentially expressed genes. Our aim in taking this approach was to describe how the host responses evolve in response to buffalo-derived *T. parva* infection. Although the presence of co-infections is possible in field studies, we confirmed the presence of *T. parva* infection in all study animals, ascertained *T. parva* as the cause of death of all cattle regarded as susceptible in this study, and confirmed the presence (Latre de Late et al., 2021) and clearance of *T. parva* parasites from the lymph nodes of all cattle that survived infection.

We used peripheral WBCs for this work. Despite the anticipated lower abundance of parasitized and responding cells in this sample type compared with the draining lymph nodes, we were still able to detect significant signals and genes that are differentially enriched at different time points and in different cattle groups. These genes can be explored further in in vitro cellular studies.

The proportion of reads unmapped to the bovine genome that aligned to the *T. parva* genome was very low at days 0 and 7, and is likely attributable to background levels of read mismapping. The source of the *T. parva*-aligned transcripts is presumably macroschizont-infected lymphocytes, as the major form found in peripheral blood in most theilerial infections is the piroplasm, which does not occur regularly in cattle infected with buffalo-derived parasites (Neitz, 1957).

The response of cattle to *T. parva* exposure is expected to represent both features of the parasite, e.g., its potential to transform and proliferate cells, and the host immune response. The *T. parva* parasite load has been associated with the clinical severity and outcome of disease in cattle (Jura and Losos, 1980; Yamada et al., 2009). We have reported previously that the animals which succumbed to *T. parva* infection in these field studies showed a lymph node parasitosis of earlier onset and greater severity (Latre de Late et al., 2021; Wragg et al., 2022). This led to the working hypothesis that the tolerant cattle limit the proliferation of infected cells. Our current results support this idea, in that there are potentially fewer *T. parva*-aligned transcripts at day 15 in the animals which survived ($P = 0.076$). Although it cannot be excluded though that these animals were infected with forms of the pathogens that proliferated less readily, the higher proportion of *T. parva* transcripts in

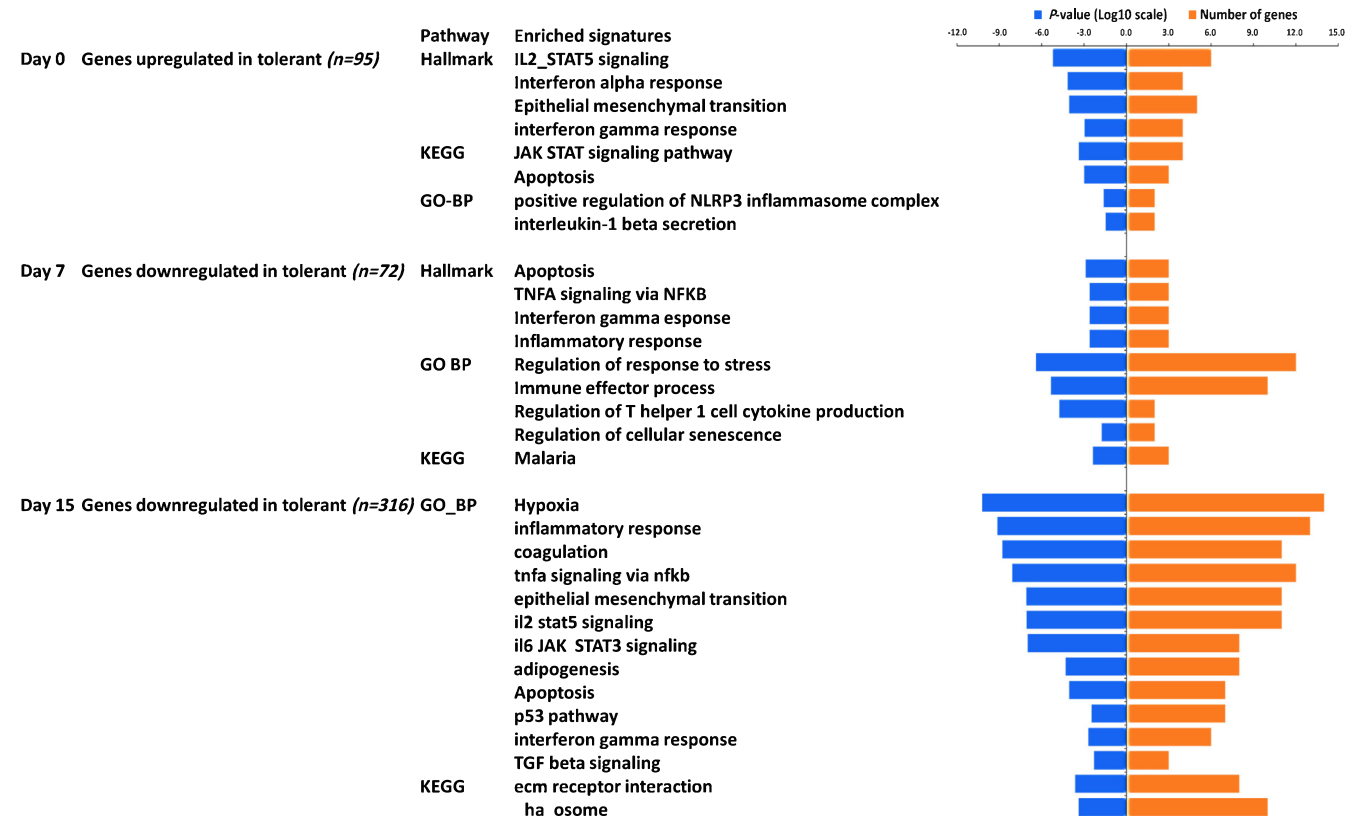

Fig. 6. Functional enrichment analysis of genes differentially expressed at the three time points in cattle that survived versus those that succumbed to infection with *Theileria parva*. The gene sets used for this analysis were termed as upregulated or downregulated in the tolerant group based on the fold change observed. Only the numbers (*n*) of genes that were either upregulated or downregulated out of all genes differentially expressed at nominal *P* value < 0.01 at each timepoint listed is given. The enriched terms were identified via functional enrichment analyses using functional mapping and annotation (FUMA) and Database for Annotation, Visualisation and Integrated Discovery (DAVID) softwares. The results of the enrichment analyses were retained if they had a false discovery rate (FDR) < 0.05. The pathways listed belong to annotations under the categories: Gene Ontology (GO) biological processes (BP), hallmark genes, and the Kyoto Encyclopaedia of Genes and Genomes (KEGG).

the animals which were treated or euthanized supports the field diagnosis that these animals were undergoing severe disease due to *T. parva* infection. As the last sequencing samples were collected on day 15 and the mean time to death or intervention was 20.4 days, it is likely that further increases in the parasite load occurred and that the proportion of *T. parva*-aligned reads observed on day 15 is an underestimate of the maximum level which occurred.

The relatively lower number of parasite transcripts derived from the tolerant cattle was not uniform, in that several susceptible cattle had fewer transcripts than some of the tolerant ones (Fig. 2A). It should be noted that the number of parasite transcripts may not be absolutely correlated to the number of infected cells. The number of transcripts detected in circulating lymphocytes depends on the number of infected cells which have migrated from the draining lymph node into the circulation, the number of parasite nuclei per cell and the overall transcriptional activity of the parasite. We cannot at this stage also exclude host genetic effects, such as a decreased sensitivity of tolerant animals to the pathogenic effects of the infected cell, to account for this seemingly anomalous observation.

Our results showed good mapping of our reads to the host genome. The divergence observed in base sequence GC content throughout the time course indicates the gross host response to infection and is possibly a result of genes with longer transcripts being expressed, as GC content is proportional to gene length, or possibly an increase in expression of broadly expressed genes such as housekeeping genes, which typically cluster in GC-rich regions (Lercher et al., 2003; Pozzoli et al., 2008). Functional annotation of GC-rich genes exhibiting the largest change in expression following infection revealed enrichment for immune-related ontologies and pathways, while among genes with low GC content the TSLP and TGF-β signalling pathways were enriched. These pathways are notable as Thymic Stromal Lymphopoietin (TSLP) plays a key role in mediating type 2 immunity (Marković and Savvides, 2020), while the production of cytokines by *Theileria*-infected lymphocytes activate c-MYC - for which TGF-β is a target and activates AP-1 - which is characteristic of *Theileria*-transformed cells (Dessauge et al., 2005b).

There was a clear difference in the expression patterns of host genes before the trial (day 0) and after exposure to the infection (days 7 and 15). Examination of the specific gene expression changes reveals clusters of genes that responded in specific patterns i.e., some were more enhanced at day 7 but not at day 15, while others were persistently enhanced from day 7 up to day 15. We identified genes that have been described to play a role in the establishment of *T. parva*-infected cells, successful cell proliferation, cell death and metastasis of cells, including: *E2F* (Tretina et al., 2020), *c-MYC* (Dessauge et al., 2005a), and *TNFα* (Guergnon et al., 2003).

We also observed genes with relatively enhanced expression on day 15 compared with days 0 and 7. These genes are associated with the functions of proliferation, cell death, metastasis, and cellular hypoxia. The main pathway highlighted from our analysis is the JAK-STAT signalling pathway, the primary role of which is in the transference of cell signals from the membrane to the nucleus, and which is essential for the functioning of cytokines and other growth factors.

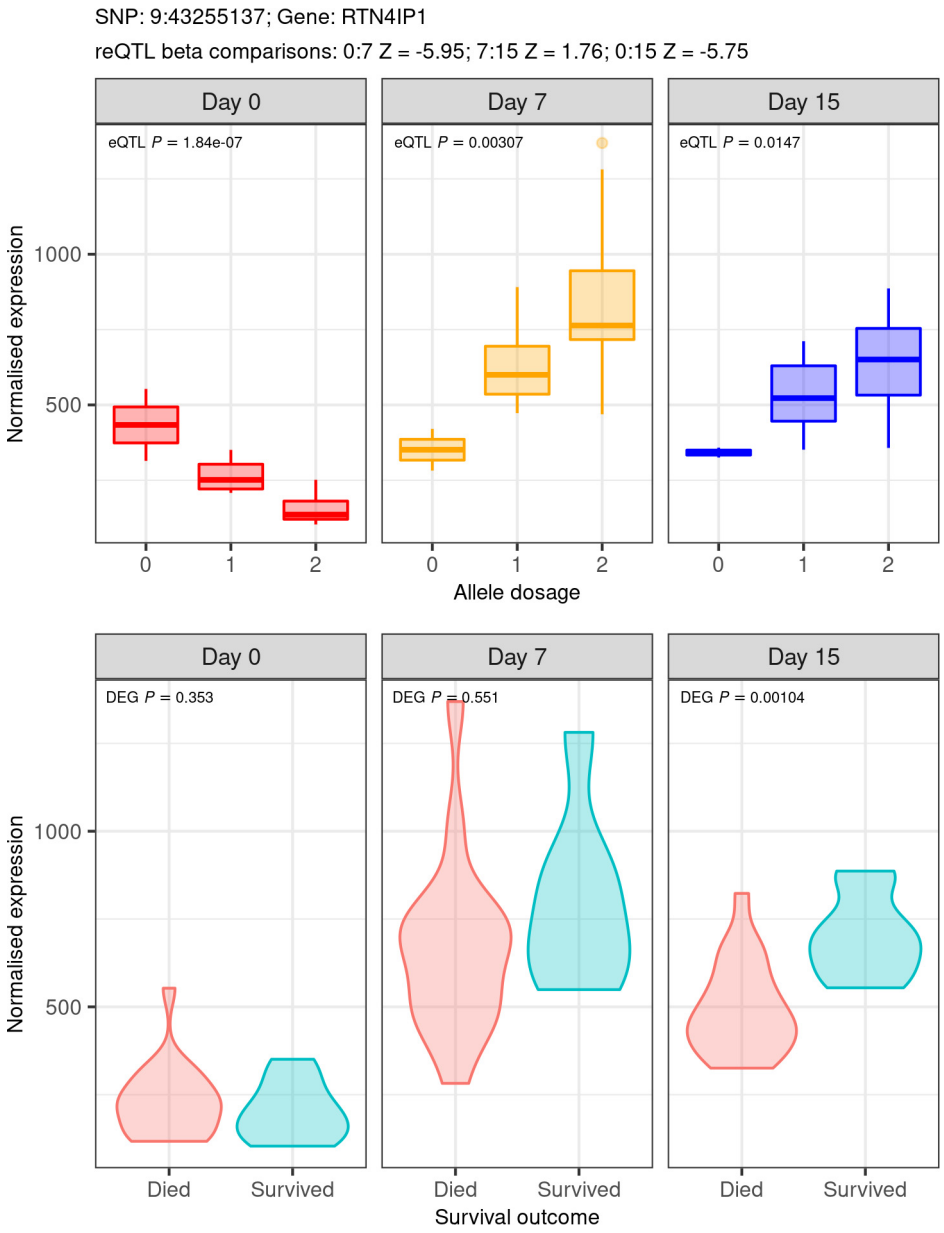

Fig. 7. Example of a significant response expression quantitative trait loci (reQTL) for *RTN4IP1*. The expression of *RTN4IP1* is significantly correlated with allele dosage at single nulcleotide polymorphism (SNP) 9:43255137. Beta comparisons indicate a significant change in the regression slope following infection of cattle with *Theileria parva*, revealing the eQTL to be a response eQTL. The expression of *RTN4IP1* is nominally significantly (ANOVA: $P < 0.05$) higher at day 15 in animals that survived infection compared with those that succumbed. RTN4IP1 was not among the significant differentially expressed genes (DEGs) following correction for multiple testing by false discovery rate (FDR).

One of the ways that *T. parva*-infected cells have been shown to evade programmed cell death is by manipulating NFkB activation. Our observation of decreasing expression of NFkB across time is contrary to previous results which described persistent induction of NFkB to be essential in *T. parva* infection as it is required for T cell activation and proliferation (Ivanov et al., 1989; Heussler et al., 1999). *Theileria parva* degrades IkB kinases in the host cell, leading to continuous translocation of NFkB to the host cell nucleus and thus prolonged cell survival (Palmer et al., 1997). The contrasting results may be due to the sample type under investigation. Most studies that have described elevated levels of NFkB used cells from in vitro cultures, in which most if not all cells are infected, whereas only a small percentage of circulating lymphocytes would be expected to be infected. This may confound the detection of NFkB transcripts in the *T. parva*-transformed cell fraction.

Investigations into which genes and functions are regulated differently during infection in cattle that are tolerant to *T. parva* infection reveals that although this group of cattle does not exhibit a distinct pattern of gene expression, they do exhibit enhanced responses that might limit cell proliferation and metastasis during infection. *KIF12* is the most significantly differentially expressed gene between tolerant and susceptible cattle, suggesting that differences in cell division (cytokinesis), and consequently proliferation between the two groups of cattle, might contribute to innate tolerance. KIF12 has not previously been identified in relation to *T. parva* pathogenesis, and is thus an avenue for future research. *RBM3* was also identified, and has been reported to play a role in cell proliferation and cell death (Wellmann et al., 2010). Another key cellular process highlighted among genes significantly differentially expressed between tolerant and susceptible cattle is

metastasis, for which *VASH1*, *HMGB3*, *IFIT1* and *TMEM213* were among the identified genes which potentially influence this cellular process.

A related publication by Latre de Late et al. (2021), using the same animals used in this study, quantified the expression of pro-inflammatory cytokines that have been previously described to have increased expression in *Theileria*-transformed cells (McGuire et al., 2004; Yamada et al., 2009). That study describes an increase in the expression of TGFβ, IL1β, IL6 and TNFα in the susceptible cattle, unlike in the tolerant cattle which maintained a relatively stable expression across time (Latre de Late et al., 2021), broadly in agreement with the observations in our study. Linking gene expression levels to the animal's genotypes, we identified a large number of regulatory variants, with links to the expression of nearby genes, which change through the course of infection. These provide potential initial indications of how the host's response to infection can depend on their genome. However, it should be noted cell type composition differences can confound these types of analyses, and future studies on isolated cell types may provide clearer insights into the genetics of the host response.

Acknowledgements

This research was funded in part by the Bill & Melinda Gates Foundation (USA) and with UK aid from the UK Foreign, Commonwealth and Development Office (Grant Agreement OPP1127286) under the auspices of the Centre for Tropical Livestock Genetics and Health (CTLGH), established jointly by the University of Edinburgh (UK), Scotland's Rural College (SRUC, UK), and the International Livestock Research Institute (Kenya). The findings and conclusions contained within are those of the authors and do not necessarily reflect positions or policies of the Bill & Melinda Gates Foundation nor the UK Government. The work was also supported by grants BBS/E/D/20002172 and BBS/E/D/20002174 from the Biotechnology and Biological Sciences Research Council (BBSRC, UK). This research was conducted as part of the Consultative Group on International Agricultural Research (CGIAR) Program on Livestock (Kenya). International Livestock Research Institute (ILRI), Kenya, is supported by contributors to the CGIAR Trust Fund. CGIAR is a global research partnership for a food-secure future. Its science is carried out by 15 Research Centres in close collaboration with hundreds of partners across the globe (www.cgiar.org). MC was supported by a fellowship No 91672938 from the German Academic exchange Service (DAAD).

Appendix A. Supplementary data

Supplementary data to this article can be found online at https://doi.org/10.1016/j.ijpara.2022.07.006.

References

Ahmed, J.S., Wiegers, P., Steuber, S., Schein, E., Williams, R.O., Dobbelaere, D., 1993. Production of interferon by *Theileria annulata*- and *T. parva*-infected bovine lymphoid cell lines. Parasitol. Res. 79, 178–182. https://doi.org/10.1007/BF00931888.

Aster, J.C., Pear, W.S., Blacklow, S.C., 2017. The varied roles of notch in cancer. Annu. Rev. Pathol. 12, 245–275. https://doi.org/10.1146/annurev-pathol-052016-100127.

Atchou, K., Ongus, J., Machuka, E., Juma, J., Tiambo, C., Djikeng, A., Silva, J.C., Pelle, R., 2020. Comparative transcriptomics of the bovine apicomplexan parasite *Theileria parva* developmental stages reveals massive gene expression variation and potential vaccine antigens. Front. Vet. Sci. 7, 287. https://doi.org/10.3389/fvets.2020.00287.

Aucan, C., Traoré, Y., Tall, F., Nacro, B., Traoré-Leroux, T., Fumoux, F., Rihet, P., 2000. High immunoglobulin G2 (IgG2) and low IgG4 levels are associated with human resistance to *Plasmodium falciparum* malaria. Infect. Immun. 68, 1252–1258. https://doi.org/10.1128/IAI.68.3.1252-1258.2000.

Bishop, R., Shah, T., Pelle, R., Hoyle, D., Pearson, T., Haines, L., Brass, A., Hulme, H., Graham, S.P., Taracha, E.L.N., Kanga, S., Lu, C., Hass, B., Wortman, J., White, O., Gardner, M.J., Nene, V., de Villiers, E.P., 2005. Analysis of the transcriptome of the protozoan *Theileria parva* using MPSS reveals that the majority of genes are transcriptionally active in the schizont stage. Nucleic Acids Res. 33, 5503–5511. https://doi.org/10.1093/nar/gki818.

Chi, H., 2012. Regulation and function of mTOR signalling in T cell fate decisions. Nat. Rev. Immunol. 12, 325–338. https://doi.org/10.1038/nri3198.

Cook, E.A.J., Sitt, T., Poole, E.J., Ndambuki, G., Mwaura, S., Chepkwony, M.C., Latre de Late, P., Miyunga, A.A., van Aardt, R., Prettejohn, G., Wragg, D., Prendergast, J.G. D., Morrison, W.I., Toye, P., 2021. Clinical evaluation of corridor disease in *Bos indicus* (Boran) cattle naturally infected with buffalo-derived *Theileria parv*a. Front. Vet. Sci. 8, 1072. https://doi.org/10.3389/fvets.2021.731238.

Critchley-Thorne, R.J., Yan, N., Nacu, S., Weber, J., Holmes, S.P., Lee, P.P., 2007. Down-regulation of the interferon signalling pathway in T lymphocytes from patients with metastatic melanoma. PLOS Med. 4, e176.

Dessauge, F., Hilaly, S., Baumgartner, M., Blumen, B., Werling, D., Langsley, G., 2005a. c-Myc activation by *Theileria* parasites promotes survival of infected B-lymphocytes. Oncogene 24, 1075–1083. https://doi.org/10.1038/sj.onc.1208314.

Dessauge, F., Lizundia, R., Baumgartner, M., Chaussepied, M., Langsley, G., 2005b. Taking the Myc is bad for *Theileria*. Trends Parasitol. 21, 377–385. https://doi.org/10.1016/j.pt.2005.06.003.

Dobbelaere, D.A.E., Fernandez, P.C., Heussler, V.T., 2000. *Theileria parva*: taking control of host cell proliferation and survival mechanisms. Cell. Microbiol. 2, 91–99. https://doi.org/10.1046/j.1462-5822.2000.00045.x.

Dobin, A., Davis, C.A., Schlesinger, F., Drenkow, J., Zaleski, C., Jha, S., Batut, P., Chaisson, M., Gingeras, T.R., 2013. STAR: ultrafast universal RNA-seq aligner. Bioinformatics 29, 15–21. https://doi.org/10.1093/bioinformatics/bts635.

Drost, H.-G., Paszkowski, J., 2017. Biomartr: genomic data retrieval with R. Bioinformatics 33, 1216–1217. https://doi.org/10.1093/bioinformatics/btw821.

Du, H., Zhao, J., Hai, L., Wu, J., Yi, H., Shi, Y., 2017. The roles of vasohibin and its family members: beyond angiogenesis modulators. Cancer Biol. Ther. 18, 827–832. https://doi.org/10.1080/15384047.2017.1373217.

Duarte, J., Deshpande, P., Guiyedi, V., Mécheri, S., Fesel, C., Cazenave, P.-A., Mishra, G. C., Kombila, M., Pied, S., 2007. Total and functional parasite specific IgE responses in *Plasmodium falciparum*-infected patients exhibiting different clinical status. Malar. J. 6, 1. https://doi.org/10.1186/1475-2875-6-1.

Eichhorn, M., Magnuson, N.S., Reeves, R., Williams, R.O., Dobbelaere, D.A., 1990. IL-2 can enhance the cyclosporin A-mediated inhibition of *Theileria parva*-infected T cell proliferation. J. Immunol. 144, 691–698.

Emery, L.D., Machugh, N.D., Morrison, W.I., 1988. *Theileria parva* (Muguga) infects bovine T-lymphocytes in vivo and induces coexpression of BoT4 and BoT8. Parasite Immunol. 10, 379–391. https://doi.org/10.1111/j.1365-3024.1988.tb00228.x.

Fry, L.M., Schneider, D.A., Frevert, C.W., Nelson, D.D., Morrison, W.I., Knowles, D.P., 2016. East coast fever caused by *Theileria parva* Is characterized by macrophage activation associated with vasculitis and respiratory failure. PLOS ONE 11, e0156004.

Gao, G., Shi, X., Long, Y., Yao, Z., Shen, J., Shen, L., 2020. The prognostic and clinicopathological significance of RBM3 in the survival of patients with tumor: A Prisma-compliant meta-analysis. Medicine (Baltimore) 99, e20002.

Guergnon, J., Chaussepied, M., Sopp, P., Lizundia, R., Moreau, M.-F., Blumen, B., Werling, D., Howard, C.J., Langsley, G., 2003. A tumour necrosis factor alpha autocrine loop contributes to proliferation and nuclear factor-κB activation of *Theileria parva*-transformed B cells. Cell. Microbiol. 5, 709–716. https://doi.org/10.1046/j.1462-5822.2003.00314.x.

Guo, S., Wang, Y., Gao, Y., Zhang, Y., Chen, M., Xu, M., Hu, L., Jing, Y., Jing, F., Li, C., Wang, Q., Zhu, Z., 2016. Knockdown of high mobility group-box 3 (HMGB3) expression inhibits proliferation, reduces migration, and affects chemosensitivity in gastric cancer cells. Med. Sci. Monit. 22, 3951–3960 https://doi.org/10.12659/MSM.900880.

Haller, D., Mackiewicz, M., Gerber, S., Beyer, D., Kullmann, B., Schneider, I., Ahmed, J. S., Seitzer, U., 2010. Cytoplasmic sequestration of p53 promotes survival in leukocytes transformed by *Theileria*. Oncogene 29, 3079–3086. https://doi.org/10.1038/onc.2010.61.

Hay, N., Sonenberg, N., 2004. Upstream and downstream of mTOR. Genes Dev. 18, 1926–1945. https://doi.org/10.1101/gad.1212704.

Heussler, V.T., Machado, J., Fernandez, P.C., Botteron, C., Chen, C.-G., Pearse, M.J., Dobbelaere, D.A.E., 1999. The intracellular parasite *Theileria parva* protects infected T cells from apoptosis. Proc. Natl. Acad. Sci. 96, 7312–7317. https://doi.org/10.1073/pnas.96.13.7312.

Heussler, V.T., Küenzi, P., Fraga, F., Schwab, R.A., Hemmings, B.A., Dobbelaere, D.A.E., 2001. The Akt/PKB pathway is constitutively activated in *Theileria*-transformed leucocytes, but does not directly control constitutive NF-κB activation. Cell. Microbiol. 3, 537–550. https://doi.org/10.1046/j.1462-5822.2001.00134.x.

Hsu, Y.-L., Shi, S.-F., Wu, W.-L., Ho, L.-J., Lai, J.-H., 2013. Protective roles of interferon-induced protein with tetratricopeptide repeats 3 (IFIT3) in dengue virus infection of human lung epithelial cells. PLOS ONE 8, e79518.

Huang, D.W., Sherman, B.T., Lempicki, R.A., 2009. Systematic and integrative analysis of large gene lists using DAVID bioinformatics resources. Nat. Protoc. 4, 44–57. https://doi.org/10.1038/nprot.2008.211.

Ito, S., Miyashita, H., Suzuki, Y., Kobayashi, M., Satomi, S., Sato, Y., 2013. Enhanced cancer metastasis in mice deficient in vasohibin-1 gene. PLOS ONE 8, e73931.

Ivanov, V., Stein, B., Baumann, I., Dobbelaere, D.A., Herrlich, P., Williams, R.O., 1989. Infection with the intracellular protozoan parasite *Theileria parva* induces

constitutively high levels of NF-kappa B in bovine T lymphocytes. Mol. Cell. Biol. 9, 4677–4686. https://doi.org/10.1128/MCB.9.11.4677.
Jura, W.G.Z., Losos, G.J., 1980. A comparative study of the diseases in cattle caused by Theileria Lawrencei and Theileria Parva. 1. Clinical signs and parasitological observations. Veterinary Parasitology 7, 275–286.
Kamau, E., Nyanjom, S.G., Wamalwa, M., Ng'ang'a,, J.,, 2016. Prediction of protein–protein interactions between *Theileria parva* and *Bos taurus* based on sequence homology. Biosci. Horiz. Int. J. Stud. Res. 9, hzw006. https://doi.org/10.1093/biohorizons/hzw006.
Katende, J., Morzaria, S., Toye, P., Skilton, R., Nene, V., Nkonge, C., Musoke, A., 1998. An enzyme-linked immunosorbent assay for detection of *Theileria parva* antibodies in cattle using a recombinant polymorphic immunodominant molecule. Parasitol. Res. 84, 408–416. https://doi.org/10.1007/s004360050419.
Kim, J., Guan, K.-L., 2019. mTOR as a central hub of nutrient signalling and cell growth. Nat. Cell Biol. 21, 63–71. https://doi.org/10.1038/s41556-018-0205-1.
Kinnaird, J.H., Weir, W., Durrani, Z., Pillai, S.S., Baird, M., Shiels, B.R., 2013. A bovine lymphosarcoma cell line infected with *Theileria annulata* exhibits an irreversible reconfiguration of host cell gene Expression. PLOS ONE 8, e66833.
Lakshmikanth, G.S., Warrick, H.M., Spudich, J.A., 2004. A mitotic kinesin-like protein required for normal karyokinesis, myosin localization to the furrow, and cytokinesis in *Dictyostelium*. Proc. Natl. Acad. Sci. 101, 16519–16524. https://doi.org/10.1073/pnas.0407304101.
Latre de Late, P., Cook, E.A.J., Wragg, D., Poole, E.J., Ndambuki, G., Miyunga, A.A., Chepkwony, M.C., Mwaura, S., Ndiwa, N., Prettejohn, G., Sitt, T., Van Aardt, R., Morrison, W.I., Prendergast, J.G.D., Toye, P., 2021. Inherited tolerance in cattle to the apicomplexan protozoan *Theileria parva* is associated with decreased proliferation of parasite-infected lymphocytes. Front. Cell. Infect. Microbiol. 11, 995. https://doi.org/10.3389/fcimb.2021.751671.
Lawrence, J.A., Perry, B.D., Williamson, S., 2004. East Coast fever. In: Coetzer, J.A.W., Tusti, R.C. (Eds.), Infectious Disease of Livestock. Oxford University Press, Cape Town, pp. 448–467.
Lercher, M.J., Urrutia, A.O., Pavlíček, A., Hurst, L.D., 2003. A unification of mosaic structures in the human genome. Hum. Mol. Genet. 12, 2411–2415. https://doi.org/10.1093/hmg/ddg251.
Liao, Y., Smyth, G.K., Shi, W., 2014. featureCounts: an efficient general purpose program for assigning sequence reads to genomic features. Bioinformatics 30, 923–930. https://doi.org/10.1093/bioinformatics/btt656.
Liu, J., Wang, L., Li, X., 2018. HMGB3 promotes the proliferation and metastasis of glioblastoma and is negatively regulated by miR-200b-3p and miR-200c-3p. Cell Biochem. Funct. 36, 357–365. https://doi.org/10.1002/cbf.3355.
Love, M.I., Huber, W., Anders, S., 2014. Moderated estimation of fold change and dispersion for RNA-seq data with DESeq2. Genome Biol. 15, 550. https://doi.org/10.1186/s13059-014-0550-8.
Ma, M., Baumgartner, M., 2014. Intracellular *Theileria annulata* promote invasive cell motility through kinase regulation of the host actin cytoskeleton. PLOS Pathog. 10, e1004003.
Mahmud, S.A., Manlove, L.S., Farrar, M.A., 2013. Interleukin-2 and STAT5 in regulatory T cell development and function. JAK-STAT 2, e23154.
Marković, I., Savvides, S.N., 2020. Modulation of signalling mediated by TSLP and IL-7 in Inflammation, autoimmune diseases, and cancer. Front. Immunol. 11, 1557. https://doi.org/10.3389/fimmu.2020.01557.
McDermott, J.E., Vartanian, K.B., Mitchell, H., Stevens, S.L., Sanfilippo, A., Stenzel-Poore, M.P., 2012. Identification and validation of Ifit1 as an important innate immune bottleneck. PLOS ONE 7, e36465.
McGuire, K., Manuja, A., Russell, G.C., Springbett, A., Craigmile, S.C., Nichani, A.K., Malhotra, D.V., Glass, E.J., 2004. Quantitative analysis of pro-inflammatory cytokine mRNA expression in *Theileria annulata*-infected cell lines derived from resistant and susceptible cattle. Vet. Immunol. Immunopathol. 99, 87–98. https://doi.org/10.1016/j.vetimm.2004.01.003.
Mikami, S., Oya, M., Kosaka, T., Mizuno, R., Miyazaki, Y., Sato, Y., Okada, Y., 2017. Increased vasohibin-1 expression is associated with metastasis and poor prognosis of renal cell carcinoma patients. Lab. Invest. 97, 854–862. https://doi.org/10.1038/labinvest.2017.26.
Miyashita, H., Watanabe, T., Hayashi, H., Suzuki, Y., Nakamura, T., Ito, S., Ono, M., Hoshikawa, Y., Okada, Y., Kondo, T., Sato, Y., 2012. Angiogenesis inhibitor vasohibin-1 enhances stress resistance of endothelial cells via induction of SOD2 and SIRT1. PLOS ONE 7, e46459.
Morrison, W.I., MacHugh, N.D., Lalor, P.A., 1996. Pathogenicity of *Theileria parva* is influenced by the host cell type infected by the parasite. Infect. Immun. 64, 557–562. https://doi.org/10.1128/iai.64.2.557-562.1996.
Musoke, A.J., Nantulya, V.M., Buscher, G., Masake, R.A., Otim, B., 1982. Bovine immune response to *Theileria parva*: neutralizing antibodies to sporozoites. Immunology 45, 663–668.
Ndungu, S.G., Ngumi, P.N., Mbogo, S.K., Dolan, T.T., Mutugi, J.J., Young, A.S., 2005. Some preliminary observations on the susceptibility and resistance of different cattle breeds to *Theileria parva* infection. Onderstepoort J. Vet. Res. 72, 7–11. https://doi.org/10.4102/ojvr.v72i1.219.
Neitz, W.O., 1957. Theileriosis, gonderioses and cytauxzoonoses: a review. Onderstepoort J. Vet. Res. 27 (3), 275–430.
Nemeth, M.J., Cline, A.P., Anderson, S.M., Garrett-Beal, L.J., Bodine, D.M., 2005. Hmgb3 deficiency deregulates proliferation and differentiation of common lymphoid and myeloid progenitors. Blood 105, 627–634. https://doi.org/10.1182/blood-2004-07-2551.
Nemeth, M.J., Kirby, M.R., Bodine, D.M., 2006. Hmgb3 regulates the balance between hematopoietic stem cell self-renewal and differentiation. Proc. Natl. Acad. Sci. 103, 13783–13788. https://doi.org/10.1073/pnas.0604006103.
Nene, V., Morrison, W.I., 2016. Approaches to vaccination against *Theileria parva* and *Theileria annulata*. Parasite Immunol. 38, 724–734. https://doi.org/10.1111/pim.12388.
Nica, A.C., Dermitzakis, E.T., 2013. Expression quantitative trait loci: present and future. Philos. Trans. R. Soc. B Biol. Sci. 368, 20120362. https://doi.org/10.1098/rstb.2012.0362.
Palmer, G.H., Machado, J., Fernandez, P., Heussler, V., Perinat, T., Dobbelaere, D.A.E., 1997. Parasite-mediated nuclear factor κB regulation in lymphoproliferation caused by *Theileria parva* infection. Proc. Natl. Acad. Sci. 94, 12527–12532. https://doi.org/10.1073/pnas.94.23.12527.
Pidugu, V.K., Pidugu, H.B., Wu, M.-M., Liu, C.-J., Lee, T.-C., 2019. Emerging functions of human IFIT proteins in cancer. Front. Mol. Biosci. 6, 148. https://doi.org/10.3389/fmolb.2019.00148.
Pilotte, J., Kiosses, W., Chan, S.W., Makarenkova, H.P., Dupont-Versteegden, E., Vanderklish, P.W., 2018. Morphoregulatory functions of the RNA-binding motif protein 3 in cell spreading, polarity and migration. Sci. Rep. 8, 7367. https://doi.org/10.1038/s41598-018-25668-2.
Pozzoli, U., Menozzi, G., Fumagalli, M., Cereda, M., Comi, G.P., Cagliani, R., Bresolin, N., Sironi, M., 2008. Both selective and neutral processes drive GC content evolution in the human genome. BMC Evol. Biol. 8, 99. https://doi.org/10.1186/1471-2148-8-99.
Raudvere, U., Kolberg, L., Kuzmin, I., Arak, T., Adler, P., Peterson, H., Vilo, J., 2019. g:Profiler: a web server for functional enrichment analysis and conversions of gene lists (2019 update). Nucleic Acids Res. 47, W191–W198. https://doi.org/10.1093/nar/gkz369.
Razmi, G., Yaghfoori, S., Mohri, M., Haghparast, A., Tajeri, S., 2019. The haematological, proinflammatory cytokines and IgG changes during an ovine experimental theileriosis. Onderstepoort J. Vet. Res. 86, 6. https://doi.org/10.4102/ojvr.v86i1.1629.
Reimand, J., Kull, M., Peterson, H., Hansen, J., Vilo, J., 2007. g:Profiler—a web-based toolset for functional profiling of gene lists from large-scale experiments. Nucleic Acids Res. 35, W193–W200. https://doi.org/10.1093/nar/gkm226.
Sager, H., Brunschwiler, C., Jungi, T.W., 1998. Interferon production by *Theileria annulata*-transformed cell lines is restricted to the beta family. Parasite Immunol. 20, 175–182. https://doi.org/10.1046/j.1365-3024.1998.00141.x.
Saxton, R.A., Sabatini, D.M., 2017. mTOR signalling in growth, metabolism, and disease. Cell 168, 960–976. https://doi.org/10.1016/j.cell.2017.02.004.
Sitt, T., Poole, E.J., Ndambuki, G., Mwaura, S., Njoroge, T., Omondi, G.P., Mutinda, M., Mathenge, J., Prettejohn, G., Morrison, W.I., Toye, P., 2015. Exposure of vaccinated and naive cattle to natural challenge from buffalo-derived *Theileria parva*. Int. J. Parasitol. Parasites Wildl. 4, 244–251. https://doi.org/10.1016/j.ijppaw.2015.04.006.
Spooner, R.L., Innes, E.A., Glass, E.J., Brown, C.G., 1989. *Theileria annulata* and *T. parva* infect and transform different bovine mononuclear cells. Immunology 66, 284–288.
Szklarczyk, D., Gable, A.L., Lyon, D., Junge, A., Wyder, S., Huerta-Cepas, J., Simonovic, M., Doncheva, N.T., Morris, J.H., Bork, P., Jensen, L.J., von Mering, C., 2019. STRING v11: protein–protein association networks with increased coverage, supporting functional discovery in genome-wide experimental datasets. Nucleic Acids Res. 47, D607–D613. https://doi.org/10.1093/nar/gky1131.
Tindih, H.S., Geysen, D., Goddeeris, B.M., Awino, E., Dobbelaere, D.A.E., Naessens, J., 2012. A *Theileria parva* isolate of low virulence infects a subpopulation of lymphocytes. Infect. Immun. 80, 1267–1273. https://doi.org/10.1128/IAI.05085-11.
Tonui, T., Corredor-Moreno, P., Kanduma, E., Njuguna, J., Njahira, M.N., Nyanjom, S.G., Silva, J.C., Djikeng, A., Pelle, R., 2018. Transcriptomics reveal potential vaccine antigens and a drastic increase of upregulated genes during *Theileria parva* development from arthropod to bovine infective stages. PLOS ONE 13, e0204047.
Tretina, K., Gotia, H.T., Mann, D.J., Silva, J.C., 2015. *Theileria*-transformed bovine leukocytes have cancer hallmarks. Trends Parasitol. 31, 306–314. https://doi.org/10.1016/j.pt.2015.04.001.
Tretina, K., Haidar, M., Madsen-Bouterse, S.A., Sakura, T., Mfarrej, S., Fry, L., Chaussepied, M., Pain, A., Knowles, D.P., Nene, V.M., Ginsberg, D., Daubenberger, C.A., Bishop, R.P., Langsley, G., Silva, J.C., 2020. *Theileria* parasites subvert E2F signalling to stimulate leukocyte proliferation. Sci. Rep. 10, 3982. https://doi.org/10.1038/s41598-020-60939-x.
Wah, S.T., Hananantachai, H., Patarapotikul, J., Ohashi, J., Naka, I., Nuchnoi, P., 2018. Interferon-induced protein with tetratricopeptide repeats 1 (IFIT1) polymorphism as a genetic marker of cerebral malaria in Thai population. Asian Pac. J. Trop. Med. 11, 376. https://doi.org/10.4103/1995-7645.234765.
Wan, J., Wu, Y., Ji, X., Huang, L., Cai, W., Su, Z., Wang, S., Xu, H., 2020. IL-9 and IL-9-producing cells in tumor immunity. Cell Commun. Signal. 18, 50. https://doi.org/10.1186/s12964-020-00538-5.
Wang, H., Deng, Q., Lv, Z., Ling, Y., Hou, X., Chen, Z., Dinglin, X., Ma, S., Li, D., Wu, Y., Peng, Y., Huang, H., Chen, L., 2019. N6-methyladenosine induced miR-143-3p promotes the brain metastasis of lung cancer via regulation of VASH1. Mol. Cancer 18, 181. https://doi.org/10.1186/s12943-019-1108-x.
Watanabe, K., Taskesen, E., van Bochoven, A., Posthuma, D., 2017. Functional mapping and annotation of genetic associations with FUMA. Nat. Commun. 8, 1826. https://doi.org/10.1038/s41467-017-01261-5.
Webster, G.A., Perkins, N.D., 1999. Transcriptional Cross Talk between NF-κB and p53. Mol. Cell. Biol. 19, 3485–3495. https://doi.org/10.1128/MCB.19.5.3485.
Wellmann, S., Truss, M., Bruder, E., Tornillo, L., Zelmer, A., Seeger, K., Bührer, C., 2010. The RNA-binding protein RBM3 is required for cell proliferation and

protects against serum deprivation-induced cell death. Pediatr. Res. 67, 35–41. https://doi.org/10.1203/PDR.0b013e3181c13326.

Wragg, D., Cook, E.A.J., de Laté, P.L., Sitt, T., Hemmink, J.D., Chepkwony, M.C., Njeru, R., Poole, E.J., Powell, J., Paxton, E.A., Callaby, R., Talenti, A., Miyunga, A.A., Ndambuki, G., Mwaura, S., Auty, H., Matika, O., Hassan, M., Marshall, K., Connelley, T., Morrison, L.J., Bronsvoort, B.M., de C, Morrison, W.I., Toye, P.G., Prendergast, J.G.D., 2022. A locus conferring tolerance to *Theileria* infection in African cattle. PLOS Genet. 18, e1010099.

Yamada, S., Konnai, S., Imamura, S., Simuunza, M., Chembensofu, M., Chota, A., Nambota, A., Onuma, M., Ohashi, K., 2009. Quantitative analysis of cytokine mRNA expression and protozoan DNA load in *Theileria parva*-infected cattle. J. Vet. Med. Sci. 71, 49–54. https://doi.org/10.1292/jvms.71.49.

Yang, W., Tanaka, Y., Bundo, M., Hirokawa, N., 2014. Antioxidant signalling involving the microtubule motor KIF12 is an intracellular target of nutrition excess in beta cells. Dev. Cell 31, 202–214. https://doi.org/10.1016/j.devcel.2014.08.028.

Zhao, G., Na, R., Li, L., Xiao, H., Ding, N., Sun, Y., Han, R., 2017. Vasohibin-1 inhibits angiogenesis and suppresses tumor growth in renal cell carcinoma. Oncol. Rep. 38, 1021–1028. https://doi.org/10.3892/or.2017.5746.

Zou, J., Li, Z., Deng, H., Hao, J., Ding, R., Zhao, M., 2019. TMEM213 as a novel prognostic and predictive biomarker for patients with lung adenocarcinoma after curative resection: a study based on bioinformatics analysis. J. Thorac. Dis. 11 https://doi.org/10.21037/jtd.2019.08.01.